Ozone at low concentrations does not affect motility and proliferation of cancer cells *in vitro*

Manuela Costanzo,[1] Alessandro Romeo,[2] Barbara Cisterna,[1] Laura Calderan,[1] Paolo Bernardi,[1] Viviana Covi,[3] Gabriele Tabaracci,[3] Manuela Malatesta[1]

[1]Department of Neurosciences, Biomedicine and Movement Sciences, University of Verona
[2]Department of Computer Science, University of Verona
[3]San Rocco Clinic, Montichiari (BS), Italy

ABSTRACT

Exposure to low ozone concentrations is used in medicine as an adjuvant/complementary treatment for a variety of diseases. The therapeutic potential of low ozone concentrations relies on their capability to increase the nuclear translocation of the Nuclear factor erythroid 2-related factor 2 (Nrf2), thus inducing the transcription of Antioxidant Response Elements (ARE)-driven genes and, through a cascade of events, a general cytoprotective response. However, based on the controversial role of Nrf2 in cancer initiation, progression and resistance to therapies, possible negative effects of ozone therapy may be hypothesised in oncological patients. With the aim to elucidate the possible changes in morphology, migration capability and proliferation of cancer cells following mild ozone exposure, we performed wound healing experiments *in vitro* on HeLa cells treated with low ozone concentrations currently used in the clinical practice. By combining a multimodal microscopy approach (light and fluorescence microscopy, scanning electron microscopy, atomic force microscopy) with morphometric analyses, we demonstrated that, under our experimental conditions, exposure to low ozone concentrations does not alter cytomorphology, motility and proliferation features, thus supporting the notion that ozone therapy should not positively affect tumour cell growth and metastasis.

Key words: Wound healing; actin; morphometry; fluorescence microscopy; atomic force microscopy; scanning electron microscopy.

Correspondence: Manuela Malatesta, Department of Neurosciences, Biomedicine and Movement Sciences, University of Verona, Strada Le Grazie 8, 37134 Verona, Italy. Tel. +39.045.8027569.
E-mail: manuela.malatesta@univr.it

Contributions: All authors contributed to the study conception and design. MC, BC, LC, PB performed experiments with the various techniques and analysed data; AR supervised atomic force microscopy experiments and analysed data; VC, GT supervised the project and interpreted data; MM supervised the project, interpreted data and wrote the first draft of the manuscript. All authors read and commented the manuscript, and approved its final version.

Conflict of interest: The authors declare no conflict of interest.

Availability of data and materials: All data generated or analyzed during this study are included in this published article.

Ethical Approval: not applicable.

Introduction

Oxygen-ozone (O_2-O_3) therapy is a modestly invasive practice used in medicine as an adjuvant/complementary treatment for a variety of diseases, and is based on the administration of low O_3 concentrations (reviews in[1,2]). Although the biological mechanisms accounting for the therapeutic effects of O_3 administration have only partially been elucidated, it is known that this highly oxidizing gas acts in a dose-dependent manner.[3,4] High O_3 doses induce a severe oxidative stress resulting in tissue inflammation and damage through the activation of the nuclear factor kappa-light-chain-enhancer of activated B cells (NF-kB); on the contrary, low doses initiate a hormetic response (*i.e.*, "the beneficial effect of a low level exposure to an agent that is harmful at high levels"[5]) leading to a cytoprotective antioxidant response. In particular, the Nuclear factor erythroid 2-related factor 2 (Nrf2), that promotes the transcription of Antioxidant Response Elements (ARE) and the consequent production of antioxidant enzymes,[6] proved to be stimulated by the low O_3 concentrations used for various therapeutic purposes.[7-13] Recently, conclusive evidence has been provided that low O_3 concentration increases the nuclear translocation of Nrf2, thus inducing the Nrf2-mediated Keap1-dependent transcription of ARE-driven genes.[14]

Thus, robust clinical indication and growing scientific data support the efficacy of O_3 therapy in various medical fields such as *e.g.*, orthopedics,[15-17] gastroenterology,[18-20] pneumology,[21,22] dentistry.[23-25] However, doubts persist about potential negative side effects of O_3 administration.

In particular, O_3 therapy is frequently applied to oncological patients due to its efficacy in reducing some adverse side effects of the anti-cancer treatments.[26-30] Possible undesired consequences of O_3 therapy in oncological patients may be hypothesized based on recent findings on the controversial role of Nrf2 in cancer initiation, progression and resistance to therapies. Hyperactivation of Nrf2 may promote tumorigenesis by multiple ways: by helping incipient tumour cells to overcome the oxidative stress, which represents a barrier against neoplastic transformation and cancer initiation;[31] by supporting aberrant cell proliferation through both the induction of a metabolic switch towards anabolic pathways[32] and the modulation of mRNA translation;[33] by promoting angiogenesis[34] and drug resistance[35] through its potent cytoprotective effect.

In fact, no negative effects have so far been reported in oncological patients following O_3 therapy (recent reviews in[36,37]); however, to our knowledge, no experimental data are presently available on the possible changes in morphology, migration capability and proliferation of cancer cells following exposure to low O_3 concentrations.

With the aim to elucidate this issue, we performed wound healing experiments *in vitro*[38] on HeLa cells exposed to the low O_3 concentrations currently used in the clinical practice. A multimodal microscopy and morphometry approach was used to investigate the cytomorphological changes, proliferation and motility of this established cancer cell line that has previously been used as a suitable experimental model to study the effects of the exposure to low O_3 concentrations at the cellular level.[14,39]

Materials and Methods

Cell culture, wound healing assay and ozone treatment

HeLa cells were grown in Dulbecco's modified Eagle medium with 10% (v/v) foetal bovine serum (FBS), 1% (w/v) glutamine, 0.5% (v/v) amphotericin B, 100 units/mL of penicillin and 100 µg/mL of streptomycin (Gibco), at 37°C in a 5% CO_2 humidified atmosphere. Cells were trypsinized (0.25% trypsin in PBS containing 0.05% EDTA) when subconfluent, and then seeded on glass coverslips in 6-multi-well microplates, for atomic force microscopy (AFM) and scanning electron microscopy (SEM), or in 24-multi-well microplates (for wound healing assay and fluorescence microscopy). For wound healing assay, $5x10^5$ cells per well were seeded on 24x24 mm slides and, after 48 h, when the cells were confluent, the cell monolayers were scratched with a sterile 200 µL pipette tips and immediately exposed to O_2-O_3 gas mixtures at two different O_3 concentrations (10 and 35 µg O_3/mL O_2) according to Costanzo *et al.*[40] A single treatment was performed since, in the clinical practice, the O_3 concentrations used for our experiments are administered once or twice a week; however, HeLa cell are rapidly dividing (their cell cycle lasts about 20 h), thus making it impossible to submit the same cells to repeated treatments without causing excessive oxidative stress. The gas was produced by an OZO2 FUTURA apparatus (Alnitec s.r.l., Cremosano, CR, Italy) which generates O_3 from medical-grade O_2, and allows photometric real-time control of gas flow rate and O_3 concentration. Cells exposed to air under the same experimental conditions served as control. To evaluate cell migration during wound healing, images at 4x magnification were taken at 0 h, 2 h, 6 h and 24 h post-treatment using an inverted microscope (Leica DMIL) equipped with an Optika Microscopes (Ponteranica, BG, Italy) camera: the cell-free area was measured in a total of 12 randomly selected microscope fields per sample (4 fields in 3 independent experiments). The progressive reduction of the cell-free area was expressed as percentage, taking as 100 % the value at time 0.

Actin staining, and evaluation of the S-phase and mitotic cell fraction

To visualize actin microfilaments, 24 h after scratching the cell monolayers the slides were fixed with 4% (v/v) formaldehyde in PBS (30 min at room temperature, RT) and 70% (v/v) ethanol in water (30 min at -20°C); after rehydration with PBS for 5 min at RT, the slides were incubated with Alexa 488-conjugated phalloidin (Molecular Probes, Invitrogen, Monza, Italy) diluted 1:40 in PBS for 1 h at RT, stained for DNA with Hoechst 33342 (0.1 µg/mL in PBS for 10 min), rinsed in PBS, and finally mounted in 1:1 PBS:glycerol.

The percentage of S-phase cells was also assessed 24 h after scratching the cell monolayers: the cells were pulse-labelled with 20 µM Bromodeoxyuridine (BrdU, Sigma-Aldrich, St. Louis, MO, USA) for 30 min at 37°C, then fixed with 70% ethanol and incubated for 20 min at RT in 2 N HCl, to denature DNA partially; after neutralization with 0.1 M sodium tetraborate (pH 8.2) for 3 min, samples were washed in PBS, permeabilized for 15 min in PBS containing 0.1 % bovine serum albumin and 0.05 % Tween-20, and incubated for 1 h with a mouse monoclonal antibody recognizing BrdU (BD, Franklin Lakes, NJ, USA) diluted 1:20 in PBS. After two washes with PBS, samples were incubated for 1 h with an Alexafluor 488-conjugated anti-mouse secondary antibody (Molecular Probes, Invitrogen, Milan), diluted 1:200. The cell samples were washed with PBS, stained for DNA with 0.1 µg/mL Hoechst 33342 in PBS for 10 min, and finally mounted in PBS:glycerol (1:1). The percentage of BrdU-positive cells was evaluated in the region located within 100 µm of the wound edge in 30 randomly-selected fields (40x) per experimental condition. The same microscopic fields were used to evaluate the mitotic index. For observation of all samples, we used an Olympus BX51 microscope equipped with a 100W mercury lamp, under the following conditions: 450-480 nm excitation filter (excf), 500 nm dichroic mirror (dm), and 515 nm barrier filter (bf) for Alexa 488; 330-385 nm excf, 400 nm dm, and 420 nm bf, for Hoechst 33342.

Images were recorded with a QICAM Fast 1394 Digital Camera (QImaging, Surrey, BC, Canada) and processed with Image-Pro Plus software (Media Cybernetics, Inc., Rockville, MD, USA).

The mean ± standard error (SE) values of the analysed variables were calculated for each experimental condition, and statistical comparisons were performed by the one-way Anova test (statistical significance was set at $p \leq 0.05$).

Scanning electron microscopy

For SEM analysis, $7x10^4$ cells per well were seeded on slides of 12 mm in diameter. After 2 h and 24 h from the scratching, the cells were fixed in 4% paraformaldehyde in PBS for 2 h at 4°C, washed in the same buffer, post-fixed with 1% OsO_4 at 4°C for 1 h, and dehydrated with acetone (Sigma-Aldrich). The samples were then treated by critical point dryer (CPD 030, Balzers), mounted on metallic specimen stubs and sputter-coated with gold (MED 010 Balzers). SEM imaging was performed by an XL30 ESEM (FEI-Philips). SEM images were used to perform quantitative evaluation of cell size and roughness. By using ImageJ software (NIH), the surface area of 50 cells per sample was measured; moreover, the cell surface facing the wound edge was measured both including and excluding cell protrusions in 10 cells per sample, the ratio between the two values was then calculated in order to obtain an index of cell surface irregularity (the higher the value the rougher the cell). Statistical evaluation of the results was performed by the one-way Anova.

Atomic force microscopy

For AFM analysis, $7x10^4$ cells per well were seeded on slides of 12 mm in diameter. For topographic images at AFM, 2 h and 24 h post-treatment the cells were fixed in 2% glutaraldehyde in phosphate buffer for 20 min, washed in the same buffer and deposited onto 20 mm mica discs (Ted Pella Inc., Redding, CA, USA), after having dried the surfaces of the slides. The mica discs were mounted on suited metallic specimen discs in order to be analysed with a NT-MDT Solver-pro equipped with a 60x60-µm scanner and gold-coated NSG-01 silicon probes, from the same company, with a curvature radius of 10 nm. To evaluate the cell thickness, the height profile was measured in 5 points (2 in the peripheral and 3 in the central region of the cell) along a line (n=25 for each experimental condition). Height values were pooled according to the different experimental conditions, the mean ± SE values were calculated and statistical comparison performed by the one-way Anova.

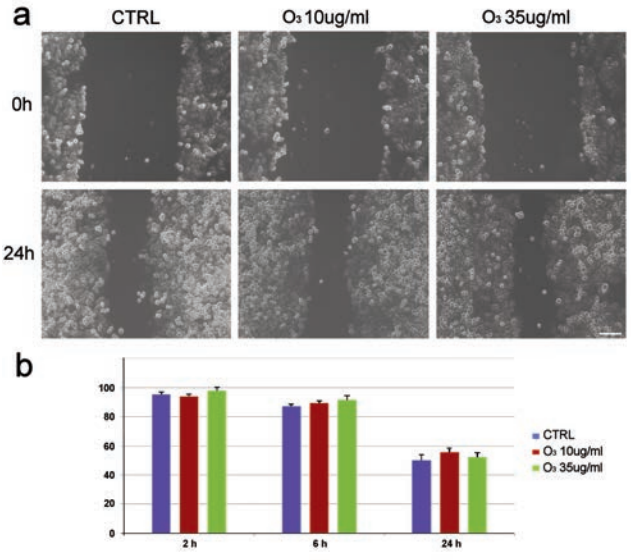

Figure 1. a) Inverted microscope images and (b) mean ± SE values of cell-free areas of control (CTRL) and O_3-treated HeLa cells at different steps of the wound healing assays. Scale bars: 100 µm.

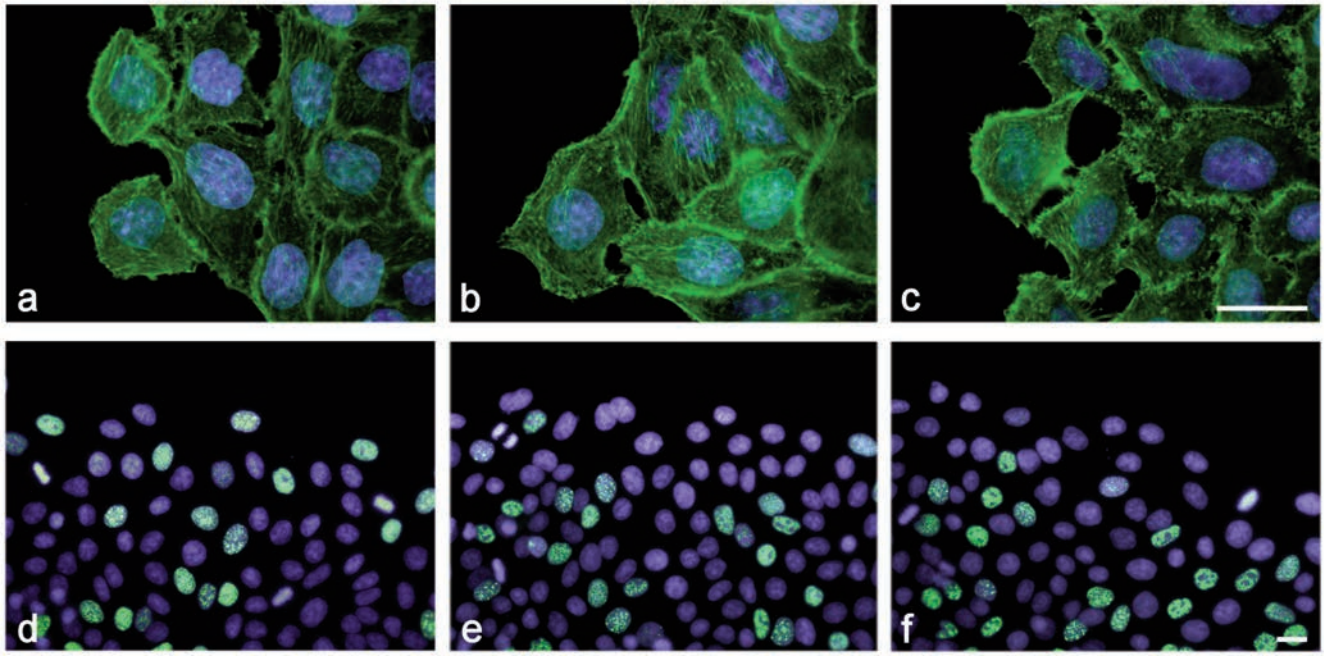

Figure 2. Fluorescence microscopy images of control (a), O_3 10 µg/mL (b) and O_3 35 µg/mL (c) treated HeLa cells labelled for actin filaments (green). Control (d), O_3 10 µg/mL (e) and O_3 35 µg/mL (f) treated HeLa cells immunolabelled for BrdU (green). DNA was counterstained with Hoechst 33342 (blue). Scale bars: 20 µm.

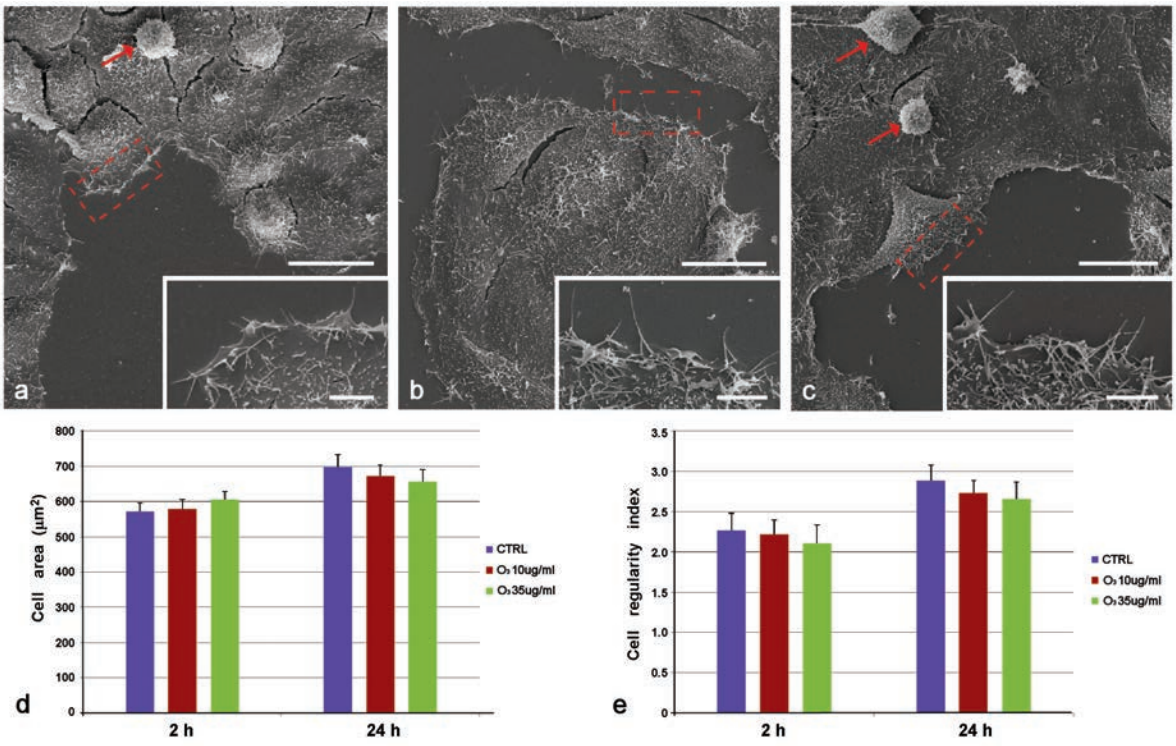

Figure 3. SEM images of control (a) O_3 10 µg/mL (b) and O^3 35 µg/mL (c) treated HeLa cells 24 h post wounding; insets: high magnification images of the dashed-line boxed areas; cell in interphase are flat with protruding microvilli, while mitotic cells (arrows) detach from the growth surface and become spherical in shape; scale bars: 25 µm; inset bars: 5 µm. Mean ± SE values of (d) cell area and (e) cell irregularity index at 2 h and 24 h from treatment; no statistical difference was found for both the cell area (2 h, P=0.605; 24 h, P=0.687) and irregularity index (2 h, P=0.850; 24 h, P=0.673).

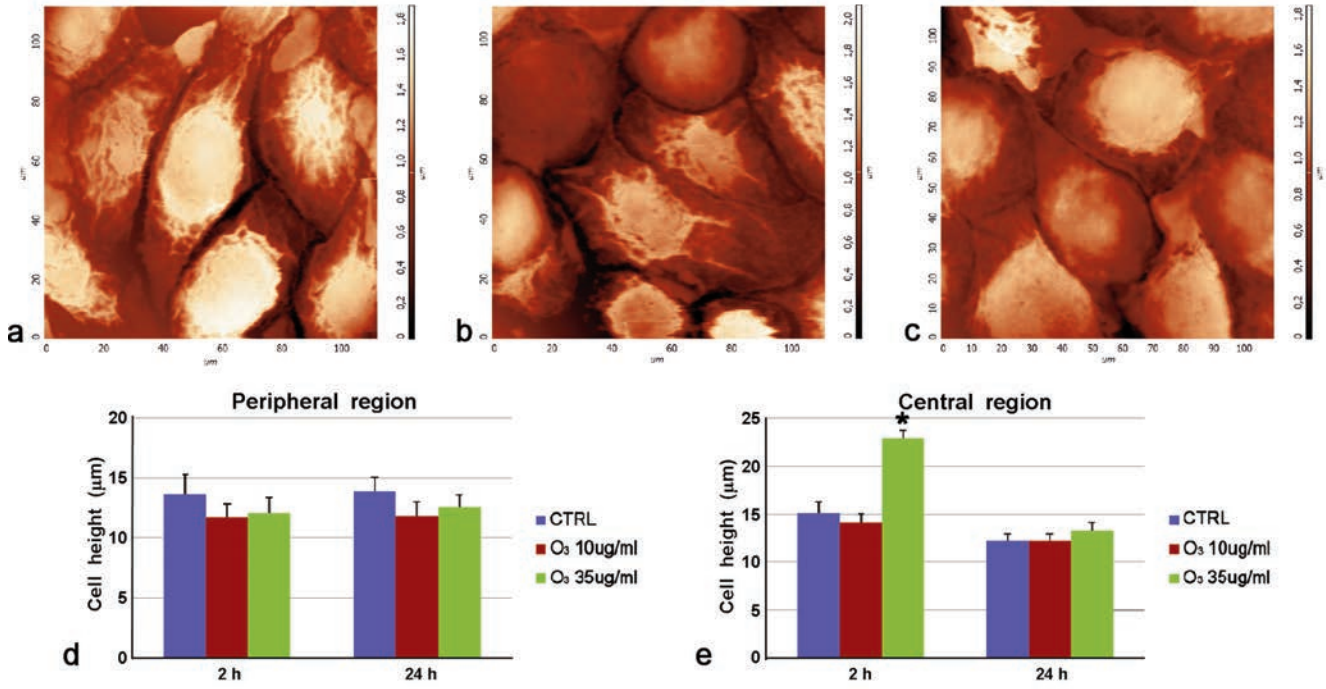

Figure 4. Representative AFM images of control (a) O_3 10 µg/mL (b) and O_3 35 µg/mL (c) treated HeLa cells 2 h post treatment. d,e) Mean ± SE values of cell height measured at AFM in control (CTRL) and in O_3-treated cells. The asterisk indicates statistical significance (P=0.002), whereas no significant difference was found among samples for the peripheral region both after 2 h and 24 h (P=0.241 and P=0.522, respectively), and for the central region after 24 h (P=0.565).

Results and Discussion

Cell movement plays a basic role in cell and tissue homeostasis as well as in many physiological and pathophysiological processes.[41] Altered regulation of cell motility is involved in several disorders, and migration of cancer cells is considered as a prerequisite for tumour metastasis.[42] Under our experimental conditions, the wound healing assay (Figure 1a) showed that the migration rates in control and O_3-treated HeLa cells were similar at each time point considered (2 h, 6 h and 24 h) after gas exposure (Figure 1b).

In eukaryotic cells, reorganization of the cytoskeletal actin is the main responsible for cell shape modification and movement by driving the protrusions that push the membrane forward and lead to pseudopod extension.[43] After fluorescent phalloidin labelling, no evident changes in actin organization were observed in migrating cells at the wound edge after O_3 exposure compared to the controls (Figure 2 a-c). This is consistent with the observations at SEM that demonstrated an unchanged morphological pattern in control and O_3-treated cells (Figure 3 a-c): in all samples, HeLa cells were flattened and irregularly polygonal in shape (apart from the sphere-shaped mitotic cells), and showed numerous filopodia and lamellipodia. The mean cell areas measured in SEM images were similar in the three experimental conditions at both 2 h and 24 h post-treatment (Figure 3d). Also the cell thickness at the peripheral and central region, as evaluated by AFM, was similar in control and O_3-treated cells (with the only exception of the cells treated with O_3 35 µg/mL after 2 h from gas exposure, that were transiently thicker than the controls in their central region) (Figure 4). Thus, O_3 treatment did not affect the volume of the cells along the wound edge, and quantitative evaluation of their surface roughness confirmed that also the surface protrusions did not significantly change (Figure 3e).

O_3 is a highly oxidizing gas and reactive oxygen species (ROS) are known to regulate cytoplasmic protrusions by controlling actin dynamics in a dose-dependent manner, high levels inducing protein depolymerization while low levels promoting polymerization.[44-46] Previous experiments[39] demonstrated that exposure to low O_3 concentrations causes a minimal ROS production, unable to induce structural or functional alterations in cell organelles including mitochondria. However, the O_3 effect on the polymerization of cytoskeletal proteins may depend on small local changes in ROS amounts. It could be therefore hypothesized that the higher oxidative stress caused by exposure to O_3 35 µg/mL may induce a transient cytoskeletal remodelling that undergoes rapid restoration without affecting the cell periphery that is mainly involved in cell movement.

Recent findings[47] suggest that cell motility is affected also by Nrf2; in fact, its repressor factor Keap1 is involved in the disassembly of podosomes, known to promote cell motility and interactions;[48] however, Keap1 is unable to play its role when tethered to Nrf2. It is worth recalling that low O_3 concentrations induce an antioxidant response by the Keap1/Nrf2 dependent pathway,[14] thus releasing free Keap1 molecules in the cytoplasm. This could explain why Nrf2 was found to play an antitumour role by reducing cell migration.[49-52]

Tumour invasion not only depends on the cell migration ability, but also on the cell proliferation rate. In previous studies, we demonstrated that exposure to low O_3 concentrations does not change both death rate[14,39] and proliferation rate of subconfluent HeLa cells[39] as well as of other cancer cell lines.[53] The present study shows that mild exposure to O_3 does not alter the percentage of BrdU-positive cells (26.92±1.47%, n=1915 in controls; 27.59±1.32%, n=1928 in cells treated with O_3 10 µg/mL $_3$; 25.81±1.36%, n=1871 in cells treated with O_3 35 µg/mL ; P=0.690) or the mitotic index (5.13±1.17% in controls, 5.81±1.05% in cells treated with O_3 10 µg/mL, and 4.62±1.23% in cells treated with O_3 35 µg/mL ; P=0.657) along the wound edge (Figure 2 d-f). These findings provide evidence that the exposure to low O_3 concentrations leaves unchanged the *in vitro* cell proliferation not only in sub-confluent populations but also during wound healing, *i.e.,* in a growth-stimulating condition.

In conclusion, the low O_3 concentrations used under *in vitro* conditions in our study proved not to alter cytomorphology, migration features or cell proliferation of HeLa cells during wound healing, thus supporting the notion that O_3 therapy should not positively affect tumour cell growth and metastasis. Especially due to the multiple indirect effects of O_3 in a living organism, the *in vivo* conditions are obviously much more complex than those of an *in vitro* model; thus, further studies are needed to clarify the consequences of the exposure to low O_3 concentrations in tumour-bearing organisms, with particular reference to the possible interference with chemotherapeutics.[36]

Acknowledgements

This work was supported by the University of Verona (Joint Projects 2017).

References

1. Viebahn-Hänsler R, León Fernández OS, Fahmy Z. Ozone in medicine: The low dose ozone concept-guidelines and treatment strategies. Ozone Sci Eng 2012;34:408-24.
2. Galiè M, Covi V, Tabaracci G, Malatesta M. The role of Nrf2 in the antioxidant cellular response to medical ozone exposure. Int J Mol Sci 2019;20 pii:E4009.
3. Bocci VA, Zanardi I, Travagli V. Ozone acting on human blood yields a hormetic dose-response relationship. J Transl Med 2011;9:66.
4. Sagai M, Bocci V. Mechanisms of action involved in ozone therapy: is healing induced via a mild oxidative stress? Med Gas Res 2011;1:29.
5. Goldman M. Cancer risk of low-level exposure. Science 1996;271:1821-2.
6. Furukawa M, Xiong Y. BTB protein Keap1 targets antioxidant transcription factor Nrf2 for ubiquitination by the Cullin 3-Roc1 ligase. Mol Cell Biol 2005;25:162-71.
7. Pecorelli A, Bocci V, Acquaviva A, Belmonte G, Gardi C, Virgili F, et al. NRF2 activation is involved in ozonated human serum upregulation of HO-1 in endothelial cells. Toxicol Appl Pharmacol 2013;267:30-40.
8. Re L, Martínez-Sánchez G, Bordicchia M, Malcangi G, Pocognoli A, Morales-Segura MA, et al. Is ozone pre-conditioning effect linked to Nrf2/EpRE activation pathway in vivo? A preliminary result. Eur J Pharmacol 2014;742:158-62.
9. Valacchi G, Sticozzi C, Zanardi I, Belmonte G, Cervellati F, Bocci V, et al. Ozone mediators effect on "in vitro" scratch wound closure. Free Radic Res 2016;50:1022-31.
10. Delgado-Roche L, Riera-Romo M, Mesta F, Hernández-Matos Y, Barrios JM, Martínez-Sánchez G, et al. Medical ozone promotes Nrf2 phosphorylation reducing oxidative stress and pro-inflammatory cytokines in multiple sclerosis patients. Eur J Pharmacol 2017;811:148-54.
11. Meng W, Xu Y, Li D, Zhu E, Deng L, Liu Z, et al. Ozone pro-

tects rat heart against ischemia-reperfusion injury: a role for oxidative preconditioning in attenuating mitochondrial injury. Biomed Pharmacother 2017;88,1090-97.
12. Wang Z, Zhang A, Meng W, Wang T, Li D, Liu Z, et al. Ozone protects the rat lung from ischemia-reperfusion injury by attenuating NLRP3-mediated inflammation, enhancing Nrf2 antioxidant activity and inhibiting apoptosis. Eur J Pharmacol 2018;835:82-93.
13. Braidy N, Izadi M, Sureda A, Jonaidi-Jafari N, Banki A, Nabavi SF, et al. Therapeutic relevance of ozone therapy in degenerative diseases: Focus on diabetes and spinal pain. J Cell Physiol 2018;233:2705-14.
14. Galiè M, Costanzo M, Nodari A, Boschi F, Calderan L, Mannucci S, et al. Mild ozonisation activates antioxidant cell response by the Keap1/Nrf2 dependent pathway. Free Radic Biol Med 2018;124:114-21.
15. Borrelli E. Mechanism of action of oxygen ozone therapy in the treatment of disc herniation and low back pain. Acta Neurochir Suppl 2011;108:123-5.
16. Muto M, Giurazza F, Silva RP, Guarnieri G. Rational approach, technique and selection criteria treating lumbar disk herniations by oxygen-ozone therapy. Interv Neuroradiol 2016;22:736-40.
17. Lopes de Jesus CC, Dos Santos FC, de Jesus LMOB, Monteiro I, Sant'Ana MSSC, Trevisani VFM. Comparison between intra-articular ozone and placebo in the treatment of knee osteoarthritis: A randomized, double-blinded, placebo-controlled study. PLoS One 2017;12:e0179185.
18. Carpendale MT, Freeberg J, Griss JM. Does ozone alleviate AIDS diarrhea? J Clin Gastroenterol 1993;17:142-5.
19. Altinel O, Demirbas S, Cakir E, Yaman H, Ozerhan I.H, Duran E, et al. Comparison of hyperbaric oxygen and medical ozone therapies in a rat model of experimental distal colitis. Scand J Clin Lab Invest 2011;71:185-92.
20. Aslaner A, Çakır T, Tekeli S, Avcı S, Doğan U, Tekeli F, et al. Medical ozone treatment ameliorates the acute distal colitis in rat. Acta Cir Bras 2016;31:256-63.
21. Hernández Rosales FA, Calunga Fernández JL, Turrent Figueras J, Menéndez Cepero S, Montenegro Perdomo A. Ozone therapy effects on biomarkers and lung function in asthma. Arch Med Res 2005;36:549-54.
22. Kucukgul A, Erdogan S, Gonenci R, Ozan G. Beneficial effects of nontoxic ozone on H2O2-induced stress and inflammation. Biochem Cell Biol 2016;94:577-83.
23. Gupta G, Mansi B. Ozone therapy in periodontics. J Med Life 2012;5:59-67.
24. Al-Omiri, MK, Abul Hassan RS, AlZarea BK, Lynch E. Comparison of dental bleaching effects of ozone and hydrogen peroxide: An ex vivo study. Am J Dent 2016;29:251-4.
25. Isler SC, Unsal B, Soysal F, Ozcan G, Peker E, Karaca IR. The effects of ozone therapy as an adjunct to the surgical treatment of peri-implantitis. J Periodontal Implant Sci 2018;48:136-51.
26. Petrucci MT, Gallucci C, Agrillo A, Mustazza MC, Foà R. Role of ozone therapy in the treatment of osteonecrosis of the jaws in multiple myeloma patients. Haematologica 2007;92:1289-90.
27. Berni F, Bolletin A, Bonfatti A, Chiamenti L, De Belardini V, De Bonis T, et al. Effectiveness of oxygen-ozone therapy as support treatment in the care of cancer patients undergoing chemo/radiotherapy (Conference Paper). Int J Ozone Ther 2013;12:38-9.
28. Clavo B, Santana-Rodriguez N, Llontop P, Gutierrez D, Ceballos D, Méndez C, et al. Ozone therapy in the management of persistent radiation-induced rectal bleeding in prostate cancer patients. Evid Based Complement Alternat Med 2015;2015:480369.
29. Velikaya VV, Gribova OV, Musabaevau U, Startseva ZhA, Simonov KA, Aleinik AN, et al. Ozone therapy for radiation reactions and skin lesions after neutron therapy in patients with malignant tumors. Voprosy Onkologii 2015;61:571-4.
30. Luongo M, Brigida AL, Mascolo L, Gaudino G. Possible therapeutic effects of ozone mixture on hypoxia in tumor development. Anticancer Res 2017;37:425-35.
31. DeNicola GM, Karreth FA, Humpton TJ, Gopinathan A, Wei C, Frese K, et al. Oncogene-induced Nrf2 transcription promotes ROS detoxification and tumorigenesis. Nature 2011;475:106-9.
32. Mitsuishi Y, Taguchi K, Kawatani Y, Shibata T, Nukiwa T, Aburatani H, et al. Nrf2 redirects glucose and glutamine into anabolic pathways in metabolic reprogramming. Cancer Cell 2012;22:66-79.
33. Chio II, Jafarnejad SM, Ponz-Sarvise M, Park Y, Rivera K, Palm W, et al. NRF2 promotes tumor maintenance by modulating mRNA translation in pancreatic cancer. Cell 2016;166: 963-76.
34. Hojo T, Maishi N, Towfik AM, Akiyama K, Ohga N, Shindoh M, et al. ROS enhance angiogenic properties via regulation of NRF2 in tumor endothelial cells. Oncotarget 2017; 8:45484-95.
35. Kang KA, Hyun JW. Oxidative stress, Nrf2, and epigenetic modification contribute to anticancer drug resistance. Toxicol Res 2017; 33:1-5.
36. Clavo B, Santana-Rodríguez N, Llontop P, Gutiérrez D, Suárez G, López L, et al. Ozone therapy as adjuvant for cancer treatment: Is further research warranted? Evid Based Complement Alternat Med 2018;2018:7931849.
37. Tirelli U, Cirrito C, Pavanello M, Del Pup L, Lleshi A, Berretta M. Oxygen-ozone therapy as support and palliative therapy in 50 cancer patients with fatigue - A short report. Eur Rev Med Pharmacol Sci 2018;22:8030-3.
38. Jonkman JEN, Cathcart JA, Xu F, Bartolini ME, Amon JE, Stevens KM, et al. An introduction to the wound healing assay using live-cell microscopy. Cell Adh Migr 2014;8:440-51.
39. Costanzo M, Cisterna B, Vella A, Cestari T, Covi V, Tabaracci G, et al. Low ozone concentrations stimulate cytoskeletal organization, mitochondrial activity and nuclear transcription. Eur J Histochem 2015;59:2515.
40. Costanzo M, Cisterna B, Covi V, Tabaracci G, Malatesta M. An easy and inexpensive method to expose adhering cultured cells to ozonization. Microscopie 2015;23:46-52. Available from: https://www.pagepressjournals.org/index.php/microscopie/article/view/5164
41. Ridley AJ, Schwartz MA, Burridge K, Firtel RA, Ginsberg MH, Gary Borisy G, et al. Cell Migration: Integrating Signals from Front to Back. Science 2003;302:1704-9.
42. Fife CM, McCarroll JA, Kavallaris M. Movers and shakers: cell cytoskeleton in cancer metastasis. Br J Pharmacol 2014;171:5507-23.
43. Huang CH, Tang M, Shi C, Iglesias PA, Devreotes PN. An excitable signal integrator couples to an idling cytoskeletal oscillator to drive cell migration. Nat Cell Biol 2013;15:1307-16.
44. Sakai J, Li J, Subramanian KK, Mondal S, Bajrami B, Hattori H, et al. Reactive oxygen species (ROS)-induced actin glutathionylation controls actin dynamics in neutrophils. Immunity 2012;37:1037-49.
45. Taulet N, Delorme-Walker VD, DerMardirossian C. Reactive oxygen species regulate protrusion efficiency by controlling actin dynamics. PLoS ONE 2012;7:e41342.
46. Muliyil S, Narasimha M. Mitochondrial ROS regulates cytoskeletal and mitochondrial remodeling to tune cell and tissue dynamics in a model for wound healing. Dev Cell 2014;28:239-52.
47. Kloska D, Kopacz A, Cysewski D, Aepfelbacher M, Dulak J,

Jozkowicz A, et al. Nrf2 sequesters Keap1 preventing podosome disassembly: a quintessential duet moonlights in endothelium. Antioxid Redox Signal 2019;30:1709-30.
48. Paterson EK, Courtneidge SA. Invadosomes are coming: new insights into function and disease relevance. FEBS J 2018;285:8-27.
49. Rachakonda G, Sekhar KR, Jowhar D, Samson PC, Wikswo JP, Beauchamp RD, et al. Increased cell migration and plasticity in Nrf2-deficient cancer cell lines. Oncogene 2010;29: 3703-14.
50. Chien MH, Lee WJ, Hsieh FK, Li CF, Cheng TY, Wang MY, et al. Keap1-Nrf2 interaction suppresses cell motility in lung adenocarcinomas by targeting the s100p protein. Clin Cancer Res 2015;21:4719-32.
51. Tertil M, Golda S, Skrzypek K, Florczyk U, Weglarczyk K, Kotlinowski J, et al. Nrf2-heme oxygenase-1 axis in mucoepidermoid carcinoma of the lung: antitumoral effects associated with down-regulation of matrix metalloproteinases. Free Radic Biol Med 2015;89:147-57.
52. Xue D, Zhou C, Shi Y, Lu H, Xu R, He X. Nuclear transcription factor Nrf2 suppresses prostate cancer cells growth and migration through upregulating ferroportin. Oncotarget 2016;7:78804-12.
53. Scassellati C, Costanzo M, Cisterna B, Nodari A, Galiè M, Cattaneo A, et al. Effects of mild ozonisation on gene expression and nuclear domains organization in vitro. Toxicol In Vitro 2017;44:100-10.

Received for publication: 23 February 2020. Accepted for publication: 19 March 2020.

European Journal of Histochemistry 2020; 64:3119
doi:10.4081/ejh.2020.3119